

PARAMETRICS OF SUBMARINE DYNAMIC STABILITY IN THE VERTICAL PLANE

Fotis A. Papoulias, Associate Professor
and
Stavros Papanikolaou, Graduate Student
Department of Mechanical Engineering
Naval Postgraduate School
Monterey, CA 93943

ABSTRACT

The problem of dynamic stability of submersible vehicles in the dive plane is examined utilizing bifurcation techniques. The primary mechanism of loss of stability is identified in the form of generic Hopf bifurcations to periodic solutions. Stability of the resulting limit cycles is established using center manifold approximations and integral averaging. Parametric studies are performed with varying vehicle geometric properties. The methods described in this work could lead to techniques resulting in enlargement of the submerged operational envelope of a vehicle.

INTRODUCTION

The dynamic response of a submersible vehicle operating at the extremes of its operational envelope is becoming increasingly important in order to enhance vehicle operations. Typically, eigenvalue analysis can be employed where the equations of motion are linearized around nominal straight line level flight paths (Arentzen and Mandel, 1960), (Clayton and Bishop, 1982), (Feldman, 1987). Under certain simplified assumptions, a simple but efficient criterion $G_v > 0$ can be obtained where the stability index G_v is a function of the hydrodynamic coefficients in heave and pitch. Values for the stability index can be computed by,

$$G_v = 1 - \frac{M_w(Z_q + m)}{Z_w M_q} . \quad (1)$$

This index is analogous to the familiar stability coefficient for horizontal plane maneuvering and can be thought of as a high speed approximation where the effect of the metacentric restoring moment is minimal.

If the value of G_v is greater than zero, the vehicle is dynamically stable. As we have established in previous studies (Papoulias and Papadimitriou, 1995) though, this is only a sufficient, and rather conservative condition for stability. Nevertheless, it is widely used and its value is indicative of vertical plane stability for any new design. We should keep in mind, however, that the condition $G_v < 0$ indicates a divergent loss of stability which is quite uncommon in the vertical plane. Most modern submarines exhibit a flutter-like instability at high speed, which can not be analyzed using the above simplified index. Divergent motions may develop in combined six degrees of freedom (Papoulias *et al*, 1993) and their occurrence can not be analyzed by a single stability index.

In our previous work (Papoulias and Papadimitriou, 1995) we examined the problem of stability of motion with controls fixed in the vertical plane, with particular emphasis on the mechanism of loss of stability of straight line motion. The closed loop control problem was analyzed in (Papoulias *et al*, 1995). The surge equation was decoupled from heave/pitch through a perturbation series approach (Bender and Orszag, 1978). It was shown that loss of stability occurs in the form of generic bifurcations to periodic solutions (Guckenheimer and Holmes, 1983). Taylor expansions and center manifold approximations were employed in order to isolate the main nonlinear terms that influence system response after the initial loss of stability (Hassard and Wan, 1978). Integral averaging was performed in order to combine the nonlinear terms into a design stability coefficient [Chow and Mallet-Paret, 1977]. Some difficulties associated with the nonsmoothness of the absolute value nonlinearities was dealt with by employing the concept of generalized gradient (Clarke, 1983). This was employed as an alternative to the linear/cubic approximation typ-

ically used in ship roll motion studies (Dalzell, 1978).

Vehicle modeling in this work follows standard notation (Gertler and Hagen, 1976), (Smith *et al.*, 1978), and numerical results are presented for a family of bodies of revolution similar to the DARPA SUBOFF model (Roddy, 1990) for which a set of hydrodynamic coefficients and geometric properties is available. This parametric study is conducted utilizing existing semi-empirical methods for the calculation of hydrodynamic coefficients. The methods are based on (Fidler and Smith, 1978), (Humphreys and Watkinson, 1978), (Peterson, 1980) and have been verified in (Wolkerstorfer, 1995). The effects of varying the nose, base, and tail fractions of the body as well its nondimensional volume to length ratio on the hydrodynamic derivatives were studied in (Holmes, 1995) where prediction equations were derived based on curve fitting of the results. These hydrodynamic prediction equations are normalized by taking the SUBOFF model as a baseline. This model has been experimentally validated for angles of attack on the hull between ± 15 deg., while the constant coefficient approximation introduces very little error in time domain simulations (Tinker, 1978). Unless otherwise mentioned, all results in this work are presented in standard dimensionless form with respect to the vehicle length $\ell = 4.26$ m, and nominal forward speed $U = 2.44$ m/sec.

PROBLEM FORMULATION

Assuming that vehicle motion is restricted in the vertical plane, the mathematical model consists of the coupled nonlinear heave and pitch equations of motion. In a moving coordinate frame fixed at the vehicle's geometrical center, Newton's equations of motion for a port/starboard symmetric and neutrally buoyant vehicle are expressed in dimensionless form as follows,

$$\begin{aligned}
m(\dot{w} - uq - z_G \dot{q}^2 - x_G \dot{q}) = & \\
Z_{\dot{q}} \dot{q} + Z_{\dot{w}} \dot{w} + Z_{qq} q + Z_w w & \\
- C_D \int_{\text{tail}}^{\text{nose}} b(x)(w - xq)|w - xq| dx, & \quad (2) \\
I_y \dot{q} + m z_G (\dot{u} + wq) - m x_G (\dot{w} - uq) = & \\
M_{\dot{q}} \dot{q} + M_{\dot{w}} \dot{w} + M_{qq} q + M_w w & \\
+ C_D \int_{\text{tail}}^{\text{nose}} b(x)(w - xq)|w - xq| x dx & \\
- x_{GB} W \cos \theta - z_{GB} W \sin \theta, & \quad (3)
\end{aligned}$$

where $x_{GB} = x_G - x_B$, $z_{GB} = z_G - z_B$, and the rest of the symbols are based on standard notation. Without loss of generality we can assume that $z_B = x_B = 0$,

so that $x_{GB} = x_G$ and $z_{GB} = z_G$. The cross flow integral terms in these equations become very important for high angles of attack maneuvering, where they provide the primary motion damping. The drag coefficient, C_D , is assumed to be constant throughout the vehicle length for simplicity. This does not affect the qualitative properties of the results that follow. The vehicle pitch rate is,

$$\dot{\theta} = q. \quad (4)$$

Dynamic coupling between surge and heave/pitch is present due to coordinate coupling as a result of the nonzero metacentric height. However, it has been shown (Papoulias and Papadimitriou, 1995) that this coupling is of higher order and does not change the linear and nonlinear results that follow.

Hydrodynamic Coefficients

Systematic studies based on semi-empirical methods have resulted in the evaluation of hydrodynamic coefficients for a generic body of revolution in terms of basic geometric properties. Curve fitting revealed that adequate accuracy for initial design can be obtained by equations of the form

$$\begin{aligned}
H_C = & A_1 F_n^2 + A_2 F_n F_m + A_3 F_m^2 + A_4 F_n \\
& + A_5 F_m + A_6 + A_7 \left(\frac{V}{L^3} - C \right),
\end{aligned}$$

where H_C denotes a given coefficient in its standard nondimensional form, V the underwater volume of the body, L its nominal length, F_n the nose fraction, and F_m the mid-body fraction. The regression coefficients A_i are as follows,

$$\begin{aligned}
Z_w & : [-0.0641, -0.1149, -0.0632, +0.0670, \\
& \quad +0.0732, -0.0263, -0.5769], \\
M_w & : [+0.0277, +0.0499, +0.0266, -0.0283, \\
& \quad -0.0301, -0.0056, -1.6357], \\
Z_q & : [-0.0314, -0.0559, -0.0292, +0.0310, \\
& \quad +0.0316, -0.0091, -0.0880], \\
M_q & : [-0.0003, +0.0040, +0.0027, -0.0012, \\
& \quad -0.0045, +0.0006, -0.1590], \\
Z_{\dot{w}} & : [+0.0002, +0.0007, +0.0007, -0.0008, \\
& \quad -0.0016, -0.0144, -1.8067], \\
M_{\dot{w}} & : [-0.0002, -0.0007, -0.0007, +0.0008, \\
& \quad +0.0016, +0.0144, +1.8067], \\
M_{\dot{q}} & : [-0.0031, -0.0046, -0.0021, +0.0031, \\
& \quad +0.0024, -0.0013, -0.0808].
\end{aligned}$$

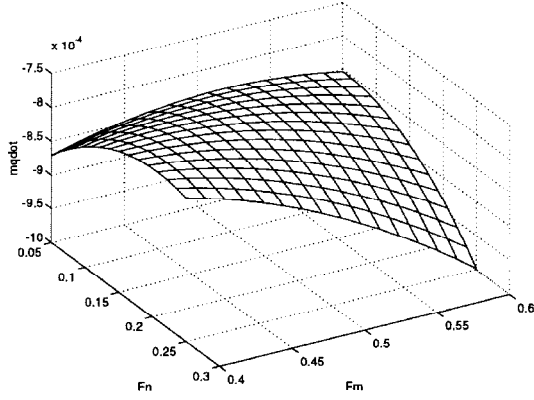


Figure 1: Hydrodynamic coefficient $M_{\dot{q}}$ versus F_n and F_m

$Z_{\dot{q}}$ was assumed constant since the semi-empirical techniques failed to compute a reliable value. The constant C is approximately 8×10^{-3} and is the nominal value for the volumetric coefficient. These expressions are for a body of revolution without appendages and assume parabolic nose, parallel mid-body, and conical tail (Holmes, 1995). Typical ranges of applicability for these regression formulas are 0.05 to 0.25 for F_n , 0.40 to 0.60 for F_m , and 6.0 to 10.0 for V/L^3 . Sample results in terms of the rotary added mass coefficient $M_{\dot{q}}$ versus the nose and mid-body fraction ratios are presented in Figure 1.

Critical Speed

The parameter value where the real part of the dominant complex conjugate pair of eigenvalues crosses zero defines the point where linear stability is lost. This critical point can be computed by considering the characteristic equation of the system. Routh's criterion applied to this can be solved for the dimensionless weight,

$$W = \frac{B_2 C_{2,0}}{A_2 D_{2,1} - B_2 C_{2,1}}, \quad (5)$$

where,

$$\begin{aligned} C_{2,0} &= Z_w(M_q - m x_G) - M_w(Z_q + m), \\ C_{2,1} &= (m - Z_w)(z_{GB} \cos \theta_0 - x_{GB} \sin \theta_0), \\ D_{2,1} &= Z_w(x_{GB} \sin \theta_0 - z_{GB} \cos \theta_0). \end{aligned}$$

It should be mentioned that the effect of the forward speed u is embedded into the definition for the dimen-

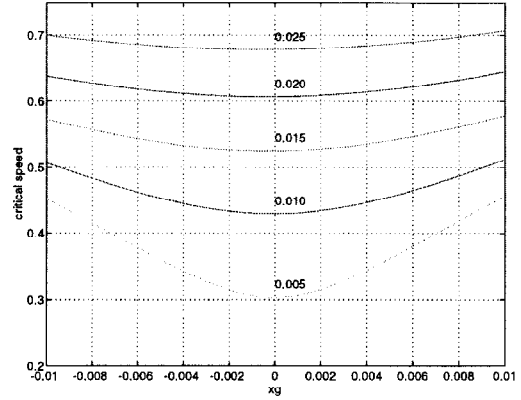


Figure 2: Critical speed for $F_n = 0.1$ and $F_m = 0.4$

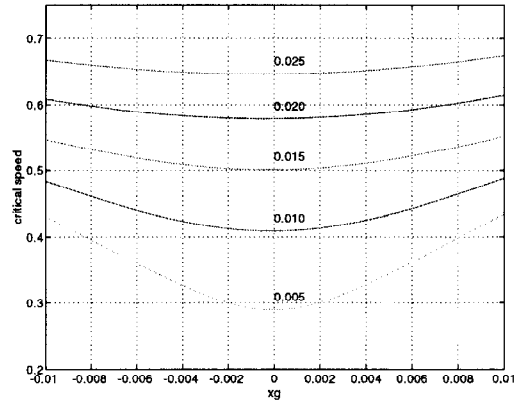


Figure 3: Critical speed for $F_n = 0.3$ and $F_m = 0.4$

sionless vehicle weight W through,

$$W \rightarrow \frac{W}{\frac{1}{2} \rho u^2 L^2}. \quad (6)$$

The value of the critical speed u_c can then be evaluated from (5) and (6). Typical results are presented in Figure 2. A family of critical speeds, u_c , is shown versus x_G with z_G as the parameter of the curves. These results were obtained for a nose fraction $F_n = 0.1$ and mid-body fraction $F_m = 0.4$. The volumetric coefficient was kept at nominal for all results. Vertical plane motions are stable for forward speeds less than the critical speed. It can be seen that stability is increasing with increasing z_G while $x_G = 0$ is the most conservative condition for stability. Therefore, a vehicle which is stable when properly trimmed will remain stable for off-trim conditions.

In order to confirm the fact that a vehicle with a longer aft-body ought to be dynamically more stable,

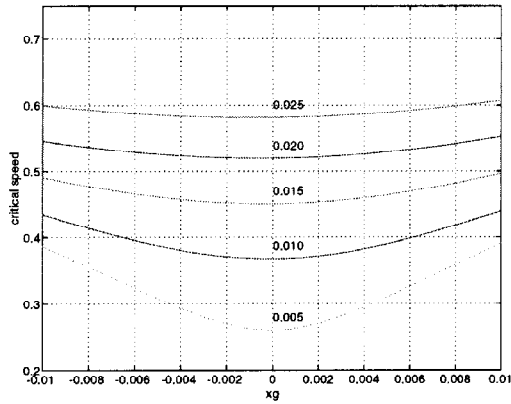


Figure 4: Critical speed for $F_n = 0.3$ and $F_m = 0.6$

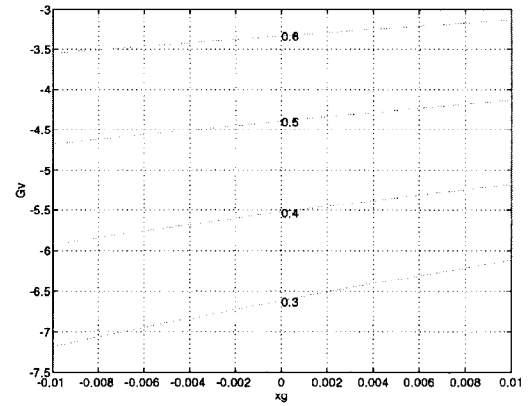


Figure 7: Stability coefficient G_v versus x_G for constant F_n and different values of F_m

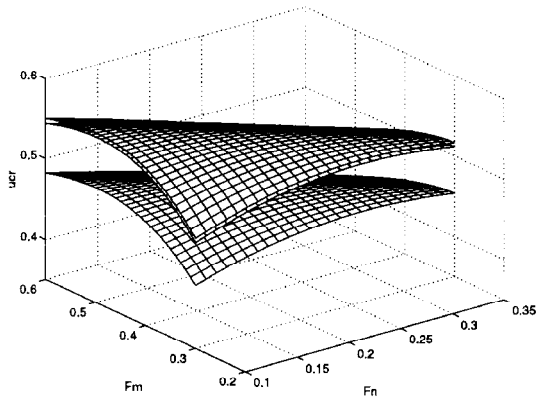


Figure 5: Critical speed versus $F_n = 0.3$ and $F_m = 0.6$ for $z_G = 0.0125$ and three values of x_G

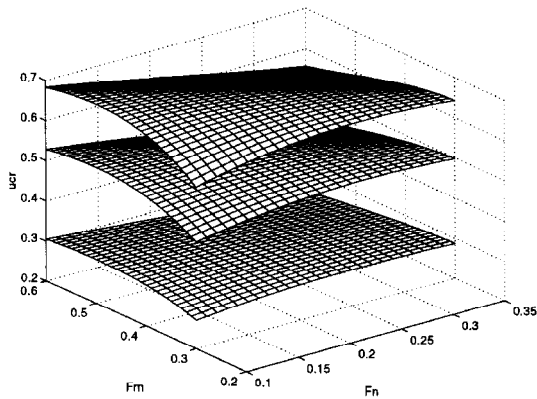


Figure 6: Critical speed versus $F_n = 0.3$ and $F_m = 0.6$ for $x_G = 0.0$ and three values of z_G

we present the results of Figures 3 and 4. The metacentric heights z_G are as in Figure 1. It can be seen that the corresponding critical speeds become smaller, thereby reducing the dynamic stability margin, as the nose and mid-body fractions are raised. This trend is consistent for all values of x_G and z_G examined.

A combined plot of the critical speed versus both F_n and F_m for $z_G = 0$ and for $x_G = (-0.01, 0, +0.01)$ is shown in Figure 5. The lower surface corresponds to $x_G = 0$. It can be seen that nonzero x_G increases the range of stability, while the general trend is to increase stability as both F_n and F_m become smaller. A similar plot for $x_G = 0$ and for three values of z_G , 0.005, 0.010, and 0.025 is shown in Figure 6. The lower surface corresponds to $z_G = 0.005$ and the higher one to $z_G = 0.025$. It can be seen that the metacentric height has by far the greatest effect on dynamic stability, while the effects of hull geometry are by comparison minimal.

A plot of the classical stability coefficient G_v from equation (1), is shown in Figure 7. The different curves correspond to various mid-body fractions, while the nose fraction is kept constant. It can be seen that G_v is negative throughout. Therefore, it would have been predicted that an unstable vehicle exists for all ranges of the parameters, which is of course incorrect. Furthermore, G_v becomes less negative as F_m is increased, which would suggest that dynamic stability is increased as the aft-body length is decreased. This is also a false conclusion. As we pointed out in the introduction, the classical stability index G_v should be used with extreme caution.

BIFURCATION ANALYSIS

In all cases of stability loss of the previous section, one pair of complex conjugate eigenvalues of the corresponding eigenvalue problem crosses transversally the imaginary axis. A situation like this in which a certain parameter is varied such that the real part of one pair of complex conjugate eigenvalues of the linearized system matrix crosses zero, results in the system leaving its steady state in an oscillatory manner. This loss of stability is called Hopf bifurcation and generically occurs in either supercritical or subcritical form. In the supercritical case, stable limit cycles are generated after the nominal straight line motion loses its stability. The amplitudes of these limit cycles are continuously increasing as the parameter distance from its critical value is increased. For small values of this criticality distance the resulting limit cycle is of small amplitude and differs little from the initial nominal state. In the subcritical case, however, stable limit cycles are generated before the nominal state loses its stability. Therefore, depending on the initial conditions it is possible to diverge away from the nominal straight line path and converge towards a limit cycle even before the nominal motion loses its stability. This means that in the subcritical Hopf bifurcation case the domain of attraction of the nominal state is decreasing and in fact shrinks to zero as the critical point is approached. Random external disturbances of sufficient magnitude can throw the vehicle off to an oscillatory steady state even though the nominal state may still remain stable. After the nominal state becomes unstable, a discontinuous increase in the magnitude of motions is observed as there exist no simple stable nearby attractors for the vehicle to converge to. Distinction between these two qualitatively different types of bifurcation is, therefore, essential in design. The computational procedure requires higher order approximations in the equations of motion and is the subject of this section.

Center Manifold Expansions

The nonlinear heave/pitch equations of motion (2), (3), and (4) are written in the form,

$$\dot{\theta} = q, \quad (7)$$

$$\dot{w} = a_{11}w + a_{12}q + a_{13}(x_{GB} \cos \theta + z_{GB} \sin \theta) + d_w(w, q) + c_1(w, q), \quad (8)$$

$$\dot{q} = a_{21}w + a_{22}q + a_{23}(x_{GB} \cos \theta + z_{GB} \sin \theta) + d_q(w, q) + c_2(w, q), \quad (9)$$

where the various coefficients are functions of the hydrodynamic derivatives and mass properties, and I_w , I_q are the cross flow integrals.

The system of equations (7) through (9) is written in the compact form

$$\dot{\mathbf{x}} = \mathbf{A}\mathbf{x} + \mathbf{g}(\mathbf{x}), \quad (10)$$

where

$$\mathbf{x} = [\theta, w, q], \quad (11)$$

is the three state variables vector, and \mathbf{A} is the linearized system matrix evaluated at the nominal point \mathbf{x}_0 . The term $\mathbf{g}(\mathbf{x})$ contains all nonlinear terms of the equations. Hopf bifurcation analysis can be performed by isolating the primary nonlinear terms in $\mathbf{g}(\mathbf{x})$. Keeping terms up to third order, we can write

$$\mathbf{g}(\mathbf{x}) = \mathbf{g}^{(2)}(\mathbf{x}) + \mathbf{g}^{(3)}(\mathbf{x}). \quad (12)$$

Using equations (7) through (11), the various terms in (12) can be written as,

$$\begin{aligned} g_1^{(2)} &= 0, \\ g_2^{(2)} &= (I_y - M_{\dot{q}})mz_G q^2 - (mx_G + Z_{\dot{q}})mz_G w q + d_w^{(2)}(w, q), \\ g_3^{(2)} &= -(m - Z_{\dot{w}})mz_G w q + (mx_G + M_{\dot{w}})mz_G q^2 + d_q^{(2)}(w, q), \end{aligned} \quad (13)$$

and

$$\begin{aligned} g_1^{(3)} &= 0, \\ g_2^{(3)} &= d_w^{(3)}(w, q) + \frac{1}{6}a_{13}(x_{GB} \sin \theta_0 - z_{GB} \cos \theta_0)\theta^3, \\ g_3^{(3)} &= d_q^{(3)}(w, q) + \frac{1}{6}a_{23}(x_{GB} \sin \theta_0 - z_{GB} \cos \theta_0)\theta^3. \end{aligned} \quad (14)$$

Expansion in Taylor series of d_w , d_q requires expansion of the cross flow integrals I_w , I_q , which require the Taylor series of

$$f(\xi) = \xi|\xi|. \quad (15)$$

This expression can be converted into an analytic function using Dalzell's approximation (Dalzell, (1978),

$$\xi|\xi| \approx \frac{5}{16}\xi_c \xi + \frac{35}{48}\frac{\xi^3}{\xi_c}, \quad (16)$$

which is derived by a least squares fit of an odd series over some assumed range of ξ , namely $-\xi_c < \xi < \xi_c$. This approximation has been extensively used in ship roll motion studies and is very useful for its intended purpose. However, in the present problem it suffers from the following drawbacks:

- It introduces a linear term which depends on the assumed range of motion, and it renders the critical speed function of the vehicle motions.
- The cubic term, which is ultimately responsible for the Hopf bifurcation analysis, is a function of the assumed range of vehicle motions which can not be known in advance.
- The slope of the actual curve at the origin is significantly different than the approximation, which would make the bifurcation results unreliable.

Instead of Dalzell's approximation, we employ the concept of generalized gradient (Clarke, (1983), which is used in the study of control systems involving discontinuous or non-smooth functions. In this way we approximate the gradient of a non-smooth function at a discontinuity by a map equal to the convex closure of the limiting gradients near the discontinuity. In our problem we write,

$$f(\xi) = \xi_0|\xi_0| + 2|\xi_0|(\xi - \xi_0) + \text{sign}(\xi_0)(\xi - \xi_0)^2 + f^{(3)}(\xi), \quad (17)$$

as the Taylor series expansion of $f(\xi)$ near ξ_0 . The sign function in (17) can be approximated by,

$$\text{sign}(\xi_0) = \lim_{\gamma \rightarrow 0} \tanh\left(\frac{\xi_0}{\gamma}\right). \quad (18)$$

The quantity γ is a small regularization parameter and is used for proper normalization of the results. Using (18), we can approximate $f(\xi)$ in the vicinity of $\xi_0 = 0$ by,

$$|\xi| \approx \frac{1}{6\gamma} \xi^3. \quad (19)$$

Since

$$\xi \mapsto w - xq, \quad (20)$$

we can express the non-smooth cross flow integral terms by,

$$I_w = \frac{C_D}{6\gamma} (E_0 w^3 - 3E_1 w^2 q + 3E_2 w q^2 - E_3 q^3),$$

$$I_q = \frac{C_D}{6\gamma} (E_1 w^3 - 3E_2 w^2 q + 3E_3 w q^2 - E_4 q^3),$$

where

$$E_i = \int_{\text{tail}}^{\text{nose}} x^i b(x) dx, \quad (21)$$

are the moments of the vehicle "waterplane" area.

Using the previous second and third order Taylor series expansions, equation (10) is written in the form,

$$\dot{\mathbf{x}} = \mathbf{A}\mathbf{x} + \mathbf{g}^{(2)}(\mathbf{x}) + \mathbf{g}^{(3)}(\mathbf{x}). \quad (22)$$

If \mathbf{T} is the matrix of eigenvectors of \mathbf{A} evaluated at the critical point $u = u_c$, the linear change of coordinates,

$$\mathbf{x} = \mathbf{T}\mathbf{z}, \quad \mathbf{z} = \mathbf{T}^{-1}\mathbf{x}, \quad (23)$$

transforms system (22) into its normal coordinate form,

$$\dot{\mathbf{z}} = \mathbf{T}^{-1}\mathbf{A}\mathbf{T}\mathbf{z} + \mathbf{T}^{-1}\mathbf{g}^{(2)}(\mathbf{T}\mathbf{z}) + \mathbf{T}^{-1}\mathbf{g}^{(3)}(\mathbf{T}\mathbf{z}). \quad (24)$$

At the Hopf bifurcation point, matrix $\mathbf{T}^{-1}\mathbf{A}\mathbf{T}$ takes the form,

$$\mathbf{T}^{-1}\mathbf{A}\mathbf{T} = \begin{bmatrix} 0 & -\omega_0 & 0 \\ \omega_0 & 0 & 0 \\ 0 & 0 & p \end{bmatrix},$$

where ω_0 is the imaginary part of the critical pair of eigenvalues, and the remaining eigenvalue p is negative. For values of u close to the bifurcation point u_c , matrix $\mathbf{T}^{-1}\mathbf{A}\mathbf{T}$ becomes,

$$\mathbf{T}^{-1}\mathbf{A}\mathbf{T} = \begin{bmatrix} \alpha'\epsilon & -(\omega_0 + \omega'\epsilon) & 0 \\ (\omega_0 + \omega'\epsilon) & \alpha'\epsilon & 0 \\ 0 & 0 & p + p'\epsilon \end{bmatrix},$$

where ϵ denotes the criticality difference

$$\epsilon = u - u_c, \quad (25)$$

and

- α' = derivative of the real part of the critical eigenvalue with respect to ϵ ,
- ω' = derivative of the imaginary part of the critical eigenvalue with respect to ϵ ,
- p' = derivative of p with respect to ϵ .

Due to continuity, the eigenvalue $p + p'\epsilon$ remains negative for small nonzero values of ϵ . Therefore, the coordinate z_3 corresponds to a negative eigenvalue and is asymptotically stable. Center manifold theory predicts that the relationship between the critical coordinates z_1, z_2 and the stable coordinate z_3 is at least of quadratic order. We can then write z_3 as,

$$z_3 = \alpha_{11}z_1^2 + \alpha_{12}z_1z_2 + \alpha_{22}z_2^2, \quad (26)$$

where the coefficients, α_{ij} , in the quadratic center manifold expansion (26) need to be determined. By differentiating equation (26) we obtain,

$$\dot{z}_3 = 2\alpha_{11}z_1\dot{z}_1 + \alpha_{12}(\dot{z}_1z_2 + z_1\dot{z}_2) + 2\alpha_{22}z_2\dot{z}_2. \quad (27)$$

We substitute $\dot{z}_1 = -\omega_0z_2$ and $\dot{z}_2 = \omega_0z_1$ and we obtain

$$\dot{z}_3 = \alpha_{12}\omega_0z_1^2 + 2(\alpha_{22} - \alpha_{11})\omega_0z_1z_2 - \alpha_{12}\omega_0z_2^2. \quad (28)$$

The third equation of (24) is written as,

$$\dot{z}_3 = pz_3 + \left[\mathbf{T}^{-1} \mathbf{g}^{(2)}(\mathbf{Tz}) \right]_{(3,3)}, \quad (29)$$

where terms up to second order have been kept. If we denote the elements of \mathbf{T} and \mathbf{T}^{-1} by,

$$\mathbf{T} = [m_{ij}], \quad \mathbf{T}^{-1} = [n_{ij}], \quad (30)$$

then

$$\mathbf{T}^{-1} \mathbf{g}^{(2)}(\mathbf{Tz}) = \begin{bmatrix} d_1 \\ d_2 \\ d_3 \end{bmatrix},$$

where expressions for d_1 , d_2 , d_3 , and the coefficients ℓ_{ij} are given in Papadimitriou (1994).

Equation (29) then becomes

$$\dot{z}_3 = pz_3 + d_3, \quad (31)$$

and substituting (26) and the expression for d_3 into (31) we get,

$$\begin{aligned} \dot{z}_3 = & (p\alpha_{11} + n_{32}\ell_{25} + n_{33}\ell_{35})z_1^2 \\ & + (p\alpha_{12} + n_{32}\ell_{26} + n_{33}\ell_{36})z_1z_2 \\ & + (p\alpha_{22} + n_{32}\ell_{27} + n_{33}\ell_{37})z_2^2. \end{aligned} \quad (32)$$

Comparing coefficients of (28) and (32) we get a system of linear equations which yields the coefficients in the center manifold expansion (26).

Using the previous Taylor expansions and center manifold approximations, we can write the reduced two-dimensional system that describes the center manifold flow of (24) in the form,

$$\begin{aligned} \dot{z}_1 = & \alpha'\epsilon z_1 - (\omega_0 + \omega'\epsilon)z_2 + F_1(z_1, z_2), \\ \dot{z}_2 = & (\omega_0 + \omega'\epsilon)z_1 + \alpha'\epsilon z_2 + F_2(z_1, z_2), \end{aligned}$$

where F_1 , F_2 are cubic polynomials in z_1 and z_2 .

If we introduce polar coordinates in the form,

$$z_1 = R \cos \phi, \quad z_2 = R \sin \phi,$$

we can produce an equation describing the rate of change of the radial coordinate R ,

$$\dot{R} = \alpha'\epsilon R + P(\phi)R^3 + Q(\phi)R^2.$$

This equation contains one variable, R , which is slowly varying in time, and another variable, ϕ , which is a fast variable. Therefore, it can be averaged over one complete cycle in ϕ to produce an equation with constant coefficients and similar stability properties,

$$\dot{R} = \alpha'\epsilon R + KR^3 + LR^2,$$

where

$$\begin{aligned} K &= \frac{1}{2\pi} \int_0^{2\pi} P(\phi) d\phi \\ &= \frac{1}{8}(3r_{11} + r_{13} + r_{22} + 3r_{24}), \\ L &= \frac{1}{2\pi} \int_0^{2\pi} Q(\phi) d\phi = 0. \end{aligned}$$

Therefore, the averaged equation becomes

$$\dot{R} = \alpha'\epsilon R + KR^3. \quad (33)$$

Equation (33) admits two steady state solutions, one at $R = 0$ which corresponds to the trivial equilibrium solution at zero, and one at

$$R_0 = \sqrt{-\frac{\alpha'}{K}\epsilon}. \quad (34)$$

This equilibrium solution corresponds to a periodic solution or limit cycle in the cartesian coordinates z_1 , z_2 . For this limit cycle to exist, the quantity R_0 must be a real number. In our case α' is always positive, since the system loses its stability; i.e., the real part of the critical pair of eigenvalues changes from negative to positive, for increasing u . Therefore, existence of these periodic solutions depends on the value of K . Specifically,

- if $K < 0$, periodic solutions exist for $\epsilon > 0$ or $u > u_c$, and
- if $K > 0$, periodic solutions exist for $\epsilon < 0$ or $u < u_c$.

The characteristic root of (33) in the vicinity of (34) is

$$\beta = -2\alpha'\epsilon, \quad (35)$$

and we can see that

- if periodic solutions exist for $u > u_c$ they are stable, and
- if periodic solutions exist for $u < u_c$ they are unstable.

Results and Discussion

Typical results of the nonlinear stability coefficient K are shown in Figures 8 and 9. The same scale has been maintained in both figures in order to facilitate direct comparison of the results. Figure 8 presents a plot of $K \cdot \gamma$ versus x_G for $z_G = 0.015$, $F_n = 0.3$, $F_m = 0.4$, and for different values of the quadratic drag coefficient C_D . It should be emphasized that the

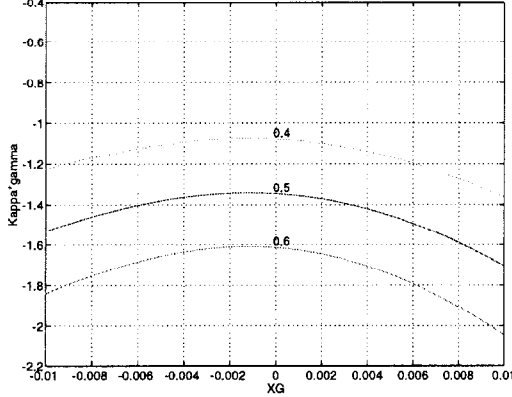


Figure 8: Nonlinear stability coefficient versus x_G for $F_n = 0.3$, $F_m = 0.6$, and different values of C_D

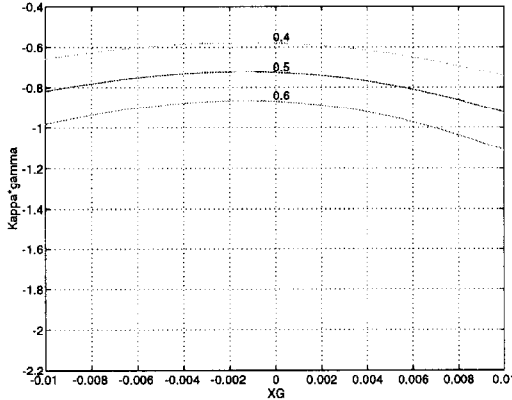


Figure 9: Nonlinear stability coefficient versus x_G for $F_n = 0.3$, $F_m = 0.4$, different values of C_D

use of $K \cdot \gamma$ is more meaningful than the use of K , since it properly accounts for the use of the regularization parameter γ . Numerical evidence suggests that all curves $K \cdot \gamma$ versus x_G converge for $\gamma \rightarrow 0$. For practical purposes, values of γ smaller than 0.001 produce identical results. The results of Figure 8 demonstrate the profound effect that the quadratic drag coefficient C_D has on stability of limit cycles. All Hopf bifurcations are supercritical ($K < 0$), and they become stronger supercritical as C_D is increased. It is worth noting that results for $C_D = 0$ produce subcritical behavior, $K > 0$, which is clearly incorrect. Thus, neglecting the effects of C_D would have produce entirely wrong results in the present problem. Additional results show that the bifurcations become stronger supercritical as initial stability z_G is increased. Figure 9 presents similar results with the only difference being the value of mid-body fraction $F_m = 0.6$. It can be seen that smaller F_m for the same F_n , which results in longer body tail, may be beneficial for stability in the linear sense but it also generates less supercritical bifurcations. This can probably be attributed to the increased responsiveness of the vehicle. It should be emphasized, however, that altering the fore and aft body lengths might influence the values of C_D which, as we pointed out, is the single most important parameter for the nonlinear nature of the bifurcations.

CONCLUDING REMARKS

This work presented a comprehensive nonlinear study of straight line stability of motion of submersibles in the dive plane under open loop conditions. A systematic perturbation analysis demonstrated that the effects of surge in heave/pitch are small and can be neglected. Primary loss of stability was shown to occur in the form of Hopf bifurcations to periodic solutions. The critical speed where instability occurs was computed in terms of metacentric height, longitudinal separation of the centers of buoyancy and gravity, and the dive plane angle. Analysis of the periodic solutions that resulted from the Hopf bifurcations was accomplished through Taylor expansions, up to third order, of the equations of motion. A consistent approximation, utilizing the generalized gradient, was used to study the non-analytic quadratic cross flow integral drag terms. The main results of this study are summarized below:

1. The critical speed of loss of stability is a monotonically increasing function of both vertical and longitudinal LCG/LCB separation. This means that

a vehicle which is stable when properly trimmed will remain stable for off-trim conditions.

2. Loss of stability occurs always in the form of supercritical Hopf bifurcations with the generation of stable limit cycles. It was found that this is mainly due to the stabilizing effects of the quadratic drag forces.
3. Even though the quadratic drag forces do not influence the initial loss of stability, they have a significant effect on post-loss of stability stabilization.
4. In general, longer aft body sections seemed to increase the range of linear stability but influence adversely the resulting limit cycles upon the initial loss of stability.

It should be emphasized that the occurrence of supercritical Hopf bifurcations is an attribute of the open loop system only. Under closed loop control, it is possible to experience either supercritical or strongly subcritical Hopf bifurcations, as shown in [Papoulias *et al* (1995)]. The latter are particularly severe in practice since self-sustained vehicle oscillations may be initiated prior to loss of stability, depending on the level of external excitation or the initial conditions.

Acknowledgments

This work was in part supported by the Naval Surface Warfare Center and the Office of Naval Research.

REFERENCES

1. Arentzen, E. S. and Mandel, P. [1960] "Naval architectural aspects of submarine design", *Trans. Soc. of Naval Archit. & Marine Engrs.*, **68**, pp. 662-692.
2. Bender, C. M. and Orszag, S. A. [1978] *Advanced Mathematical Methods for Scientists and Engineers* (McGraw-Hill, New York).
3. Chow, S.-N. and Mallet-Paret, J. [1977] "Integral averaging and bifurcation", *Journal of Differential Equations*, **26**, pp. 112-159.
4. Clayton, B. R. and Bishop, R. E. D. [1982] *Mechanics of Marine Vehicles* (Gulf Publishing Company, Houston).
5. Clarke, F. [1983] *Optimization and Nonsmooth Analysis* (Wiley and Sons, New York).
6. Dalzell, J. F. [1978] "A note on the form of ship roll damping", *Journal of Ship Research*, **22**, 3.
7. Feldman, J. [1987] Straightline and rotating arm captive-model experiments to investigate the stability and control characteristics of submarines and other submerged vehicles. Carderock Division, Naval Surface Warfare Center, Report DTRC/SHD-0303-20.
8. Fidler J. and Smith C. [1978] Methods for predicting submersible hydrodynamic characteristics. Naval Coastal Systems Center, Report TM-238-78.
9. Gertler, M. and Hagen, G. R. [1967] Standard equations of motion for submarine simulation. David Taylor Research Center, Report 2510.
10. Guckenheimer, J. and Holmes, P. [1983] *Nonlinear Oscillations, Dynamical Systems, and Bifurcations of Vector Fields* (Springer-Verlag, New York).
11. Hassard, B. and Wan, Y.H. [1978] "Bifurcation formulae derived from center manifold theory", *Journal of Mathematical Analysis and Applications*, **63**, pp. 297-312.
12. Holmes, E. P. [1995] Prediction of hydrodynamic coefficients utilizing geometric considerations. Master's Thesis, Naval Postgraduate School, Monterey, California.
13. Humphreys, D. E. and Watkinson, K. [1978] Prediction of acceleration hydrodynamic coefficients for underwater vehicles from geometric parameters. Naval Coastal Systems Laboratory, Report TR-327-78.
14. Papadimitriou, H. I. [1994] A nonlinear study of open loop dynamic stability of submersible vehicles in the dive plane. Master of Science in Mechanical Engineering and Mechanical Engineer's Thesis, Naval Postgraduate School, Monterey, California.
15. Papoulias F. A., Aydin, I., and McKinley, B. D. [1993] "Characterization of steady state solutions of submarines under casualty conditions", in *Nonlinear Dynamics of Marine Vehicles* (J. M. Falzarano, F. A. Papoulias, eds.), (ASME, New York).

16. Papoulias F. A., Bateman, C. A., and Ornek, S. [1995] "Dynamic loss of stability in depth control of submersible vehicles", *Journal of Applied Ocean Research*, **17**, 6.
17. Papoulias, F. A. and Papadimitriou, H. A. [1995] "Nonlinear studies of dynamic stability of submarines in the dive plane", *Journal of Ship Research*, **39**, 4.
18. Peterson, R. S. [1980] Evaluation of semi-empirical methods for predicting linear static and rotary hydrodynamic coefficients. Naval Coastal Systems Center, Report TM-291-80.
19. Roddy, R. F. [1990] Investigation of the stability and control characteristics of several configurations of the DARPS SUBOFF model (DTRC model 5470) from captive-model experiments. Carderock Division, Naval Surface Warfare Center, Report DTRC/SHD-1298-08.
20. Smith, N. S., Crane, J. W., and Summey, D. C. [1978] SDV simulator hydrodynamic coefficients. Naval Coastal Systems Center, Report NCSC-TM231-78.
21. Tinker, S. J. [1978] "Fluid memory effects on the trajectory of a submersible", *International Shipbuilding Progress*, **25**, 290.
22. Wolkerstorfer, W. J. [1995] A linear maneuvering model for simulation of Slice hulls. Master's Thesis, Naval Postgraduate School, Monterey, California.